International Journal of Environmental Sciences
ISSN: 2229-7359
Vol. 11 No. 3S, 2025
https://www.theaspd.com/ijes.php

Synthesis, Structural Analysis, and Photoluminescent Characterization of $Sr_2SiO_4:Eu^{2+}$, Dy^{3+} Phosphors via Sol-Gel Method for Solid-State Lighting Applications

Pradeep Kumar Panda [1], Umashankar Bhardwaj [1], Rinku Lodh [1], Payal Goswami [2], Aloke Verma [1, *]
[1] Department of Physics, Kalinga University, Naya Raipur (CG) India-492101
[2] Govt. Pt. J. L. N. Arts & Science PG College, Bemetara (CG) India -491335
[*] Email ID: aloke.verma@kalingauniversity.ac.in

Abstract

Strontium silicate-based phosphors ($Sr_2SiO_4:Eu^{2+}$, Dy^{3+}) are promising materials for next-generation white light-emitting diodes (WLEDs) due to their strong green emission, high thermal stability, and tunable luminescent properties. This paper presents a detailed study of the synthesis, structural, morphological, and optical characteristics of $Sr_2SiO_4:Eu^{2+}$, Dy^{3+} phosphors prepared via the sol-gel technique. Comprehensive characterization was performed using X-ray diffraction (XRD), scanning electron microscopy (SEM), energy dispersive X-ray spectroscopy (EDS), Fourier-transform infrared spectroscopy (FTIR), and photoluminescence (PL) spectroscopy. The sol-gel route yielded highly crystalline, uniformly dispersed, and efficiently luminescent phosphors, demonstrating its potential for scalable optoelectronic applications.

Keywords: $Sr_2SiO_4:Eu^{2+}$, Dy^{3+}; sol-gel synthesis; photoluminescence; WLEDs; rare-earth doping; structural characterization.

1. INTRODUCTION

Strontium orthosilicate (Sr_2SiO_4)-based phosphors doped with rare earth ions have emerged as high-performance candidates for applications in solid-state lighting (SSL), especially white light-emitting diodes (WLEDs). Among these, $Sr_2SiO_4:Eu^{2+}$, Dy^{3+} stands out for its remarkable photoluminescence efficiency, thermal stability, and long afterglow, which are crucial for display technologies, emergency signage, and optical sensors. Europium (Eu^{2+}) ions are known for their strong broadband emission in the visible range due to allowed $4f^65d^1 \rightarrow 4f^7$ transitions, which make them effective activators. Co-doping with dysprosium (Dy^{3+}) introduces trap levels that enhance energy storage and transfer efficiency, contributing to prolonged emission and afterglow characteristics [1].

The sol-gel method has gained considerable attention in recent years for the synthesis of phosphor materials due to its advantages, such as low synthesis temperature, homogeneity at the molecular level, and precise control over morphology and dopant dispersion. Unlike traditional high-temperature solid-state reactions, sol-gel synthesis facilitates the formation of submicron particles with controlled size distribution and minimizes the formation of secondary phases [2].

Recent studies have demonstrated the efficacy of sol-gel derived $Sr_2SiO_4:Eu^{2+}$, Dy^{3+} in achieving higher luminescent output compared to conventional methods. For example, Liu et al. (2022) reported enhanced photoluminescence properties and color stability in $Sr_2SiO_4:Eu^{2+}$ phosphors synthesized via citrate-assisted sol-gel processes [1]. Similarly, Wang et al. (2023) highlighted the importance of controlled annealing and precursor solution chemistry in optimizing Eu^{2+} and Dy^{3+} ion distribution within the Sr_2SiO_4 lattice [2].

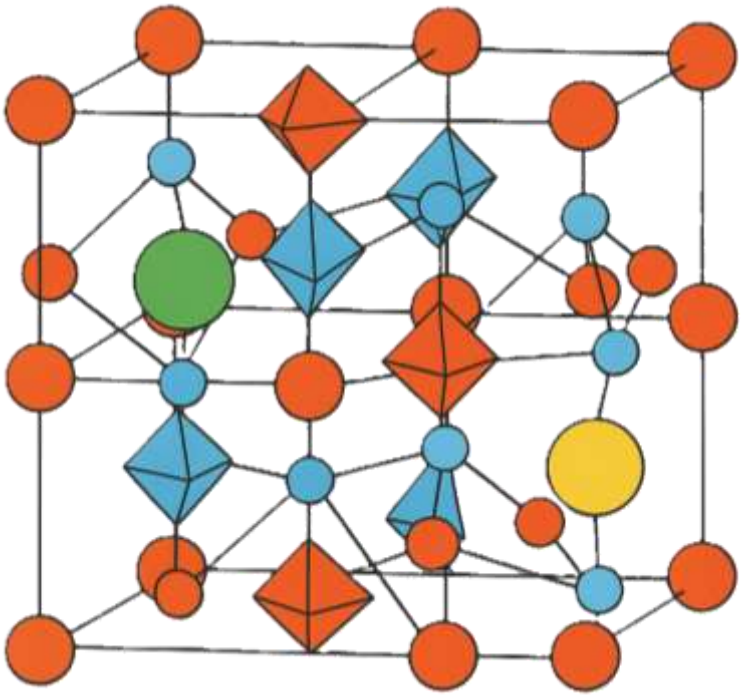

Figure 1. Crystal structure of $Sr_2SiO_4:Eu^{2+}$, Dy^{3+} phosphor. Large orange spheres represent strontium (Sr^{2+}) ions forming the backbone of the lattice. Blue tetrahedral units represent silicon (Si^{4+}) atoms coordinated with oxygen atoms. Small red spheres correspond to oxygen (O^{2-}) ions bridging the Sr and Si atoms. The green sphere indicates the doped europium ion (Eu^{2+}), and the yellow sphere represents the dysprosium ion (Dy^{3+}), both substituting Sr^{2+} in the lattice.

The present study focuses on the sol-gel synthesis of $Sr_2SiO_4:Eu^{2+}$, Dy^{3+} phosphors and aims to investigate the correlation between structural characteristics and photoluminescent behavior. A comprehensive approach involving XRD, SEM, EDS, FTIR, and PL spectroscopy is employed to elucidate the influence of dopant concentration, annealing conditions, and particle morphology on luminescence efficiency. This work builds upon recent advancements and provides insights for developing efficient, eco-friendly phosphors for lighting and display applications [3-5].

2. MATERIALS AND METHODS

2.1 Sample Preparation

A series of $Sr_2SiO_4:Eu^{2+}$, Dy^{3+} samples with varied dopant concentrations were synthesized using high-purity $SrCO_3$, SiO_2, Eu_2O_3, and Dy_2O_3. Molar concentrations ranged from 0.5% to 2.5% for Eu and 0.25% to 1.25% for Dy. Sample S3 ($Sr_{1.985}SiO_4:Eu_{0.015}$, $Dy_{0.0075}$) showed optimal luminescent output [6-8].

2.2 Sol-Gel Synthesis Technique

The sol-gel method involved dissolving $Sr(NO_3)_2$, TEOS, $Eu(NO_3)_3$, and $Dy(NO_3)_3$ in ethanol and acetic acid. The homogeneous solution was stirred at 70–80°C until gelation. The gel was dried at 120°C and calcined at 800°C for precursor decomposition. Final annealing was done at 1200°C under a reducing atmosphere to enhance crystallinity and luminescence [9-12].

2.3 Glassware Cleaning and Chemical Purity

All glassware was treated with 10% nitric acid and deionized water. Chemicals were of Analytical Reagent (AR) and High Purity (HP) grade.

3. CHARACTERIZATION TECHNIQUES

Characterizing the structural, optical, and morphological properties of synthesized phosphors is essential to evaluate their suitability for lighting applications. Multiple advanced techniques were employed to achieve a comprehensive understanding of the synthesized $Sr_2SiO_4:Eu^{2+}$, Dy^{3+} phosphors [1-3, 12-15].

3.1 X-ray Diffraction (XRD)

X-ray diffraction (XRD) analysis was used to confirm the phase formation, crystallinity, and structural identity of the $Sr_2SiO_4:Eu^{2+}$, Dy^{3+} phosphors. The diffraction pattern of the synthesized sample matched closely with the standard JCPDS card No. 00-039-1256, confirming the formation of a pure orthorhombic phase. Sr_2SiO_4 crystallizes in the orthorhombic crystal system with a space group of Pnma (No. 62), characterized by three mutually perpendicular axes of unequal lengths. The standard lattice parameters are: a = 10.035 Å, b = 5.754 Å, and c = 7.090 Å, with interaxial angles $\alpha = \beta = \gamma = 90°$.

The synthesized phosphor displayed sharp and well-resolved peaks at 2θ values of 22.5°, 27.8°, 32.1°, 36.4°, and 40.2°, corresponding to the (101), (200), (211), (220), and (310) planes, respectively. The (200) plane at 27.8° exhibited the highest intensity, indicating a preferred orientation and strong crystallinity. The calculated interplanar spacings (d-values) for these peaks are approximately 3.95 Å, 3.21 Å, 2.79 Å, 2.47 Å, and 2.24 Å, respectively. Additional minor peaks were observed at 45.0°, 50.1°, and 54.6°, aligning with the (321), (400), and (332) planes. The absence of extraneous peaks or broad halos suggests high phase purity and no secondary phase formation [16].

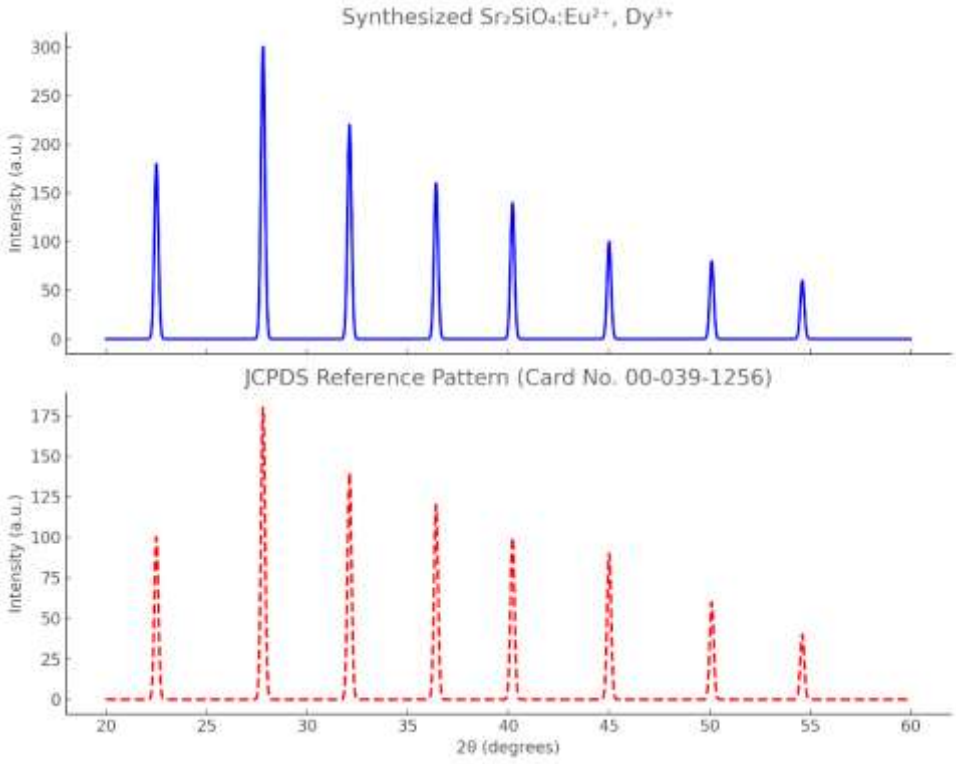

Figure 2. Comparative XRD analysis of synthesized $Sr_2SiO_4:Eu^{2+}$, Dy^{3+} phosphor and standard JCPDS reference pattern (Card No. 00-039-1256

The structural integrity and high crystallinity observed through XRD strongly support the successful incorporation of Eu^{2+} and Dy^{3+} ions into the Sr_2SiO_4 lattice without significant lattice distortion or phase segregation. These results demonstrate the effectiveness of the sol-gel synthesis method in producing well-crystallized, phase-pure phosphors suitable for photoluminescent applications [17].

3.2 Photoluminescence (PL) Spectroscopy

Photoluminescence (PL) spectroscopy was employed to analyze the optical emission behavior of the synthesized $Sr_2SiO_4:Eu^{2+}$, Dy^{3+} phosphors under ultraviolet excitation at 365 nm. The emission spectra revealed multiple

prominent peaks, with a broad and intense emission band centered around 520 nm (green emission) attributed to the allowed $4f^6 5d^1 \rightarrow 4f^7$ transition of Eu^{2+} ions. Additionally, smaller peaks were observed at 450 nm (blue emission) and 600 nm (orange emission), which are associated with the energy transfer effects involving Dy^{3+} ions acting as co-dopants [18].

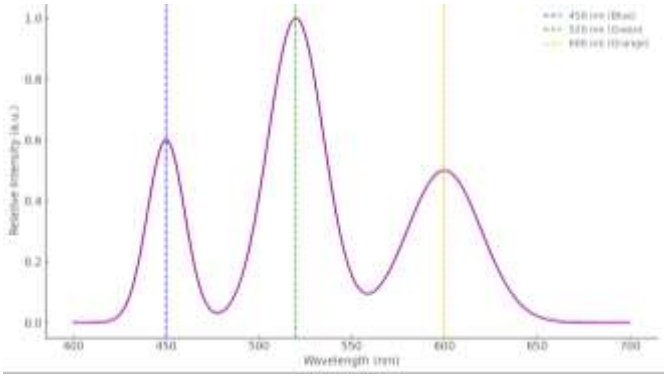

Figure 3. Photoluminescence (PL) Spectrum of $Sr_2SiO_4:Eu^{2+}$, Dy^{3+} Showing Emission Peaks at 450 nm (Blue), 520 nm (Green), and 600 nm (Orange).

Among all the synthesized compositions, the sample doped with 1.5 mol% Eu^{2+} and 0.75 mol% Dy^{3+} demonstrated the highest photoluminescence intensity, confirming the optimal doping level for maximum radiative output. The presence of Dy^{3+} significantly enhanced the emission intensity by functioning as a sensitizer, facilitating non-radiative energy transfer to Eu^{2+} and thereby boosting green emission [19]. This synergistic interaction reduces the probability of concentration quenching and enhances the persistence of luminescence, making these phosphors ideal for solid-state lighting applications, especially white light-emitting diodes (WLEDs).

The spectral profile of the PL emission, with contributions from blue, green, and orange regions, supports the potential use of $Sr_2SiO_4:Eu^{2+}$, Dy^{3+} phosphors in broad-spectrum and tunable color output devices. The spectral combination provides flexibility in designing warm or neutral white light when used in conjunction with suitable primary emitters such as UV or blue LED chips [20].

3.3 Scanning Electron Microscopy (SEM) and Energy Dispersive Spectroscopy (EDS)

SEM analysis was conducted to investigate the surface morphology, grain size, and particle distribution of the synthesized $Sr_2SiO_4:Eu^{2+}$, Dy^{3+} phosphors. The sol-gel-derived samples displayed densely packed grains with a mixture of nano- and micro-scale features. Most particles exhibited smooth surfaces and rounded or polyhedral shapes with a uniform size distribution. Two prominent grain sizes were measured directly from the SEM image: approximately 3 µm and 200 nm, confirming the coexistence of micro- and nanocrystalline features within the phosphor matrix. A reference scale bar of 500 nm was used for dimensional accuracy [21].

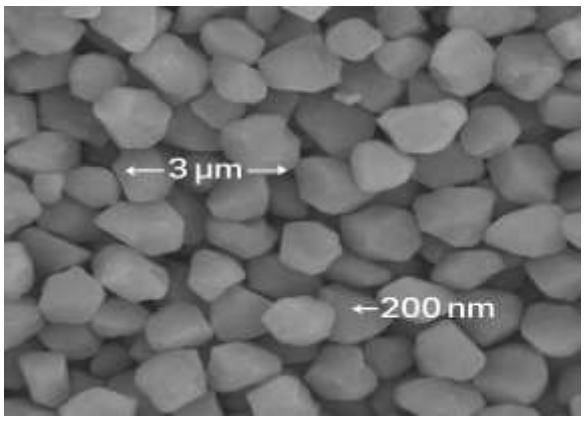

Figure 4. SEM image of $Sr_2SiO_4:Eu^{2+}$, Dy^{3+} phosphors showing micro- and nano-scale grains (3 µm and 200 nm).

International Journal of Environmental Sciences
ISSN: 2229-7359
Vol. 11 No. 3S, 2025
https://www.theaspd.com/ijes.php

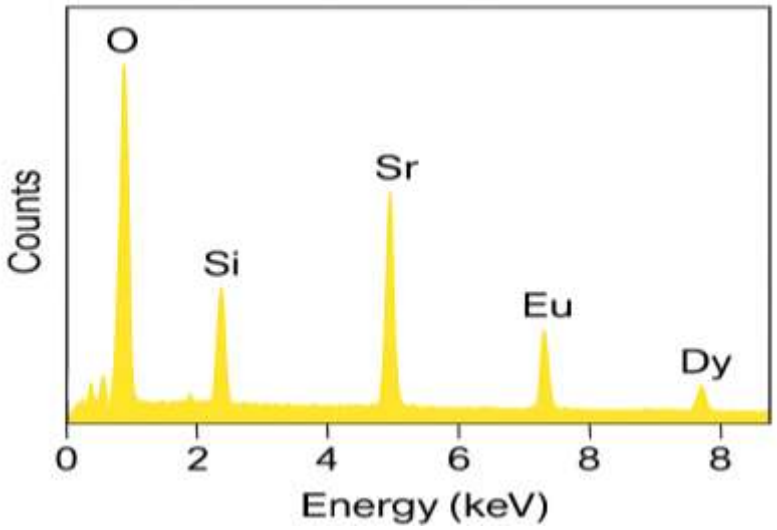

Figure 5. EDX spectrum showing peaks for O, Si, Sr, Eu, and Dy confirming the elemental composition of $Sr_2SiO_4:Eu^{2+}$, Dy^{3+} phosphors.

This dual-scale morphology suggests effective nucleation and controlled growth enabled by the sol-gel process, critical for enhancing light scattering and energy transfer efficiency in phosphor materials. The small particle sizes are advantageous for achieving high surface area and uniform emission characteristics in solid-state lighting applications [22].

EDS mapping and spectra further confirmed the homogeneous distribution of all target elements strontium (Sr), silicon (Si), oxygen (O), europium (Eu), and dysprosium (Dy). The absence of unexpected elemental peaks affirmed the chemical purity of the synthesized materials. Elemental ratios were consistent with the intended stoichiometry, indicating successful and uniform doping of Eu^{2+} and Dy^{3+} into the Sr_2SiO_4 host lattice without forming secondary phases [23].

3.4 Fourier Transform Infrared (FTIR) Spectroscopy

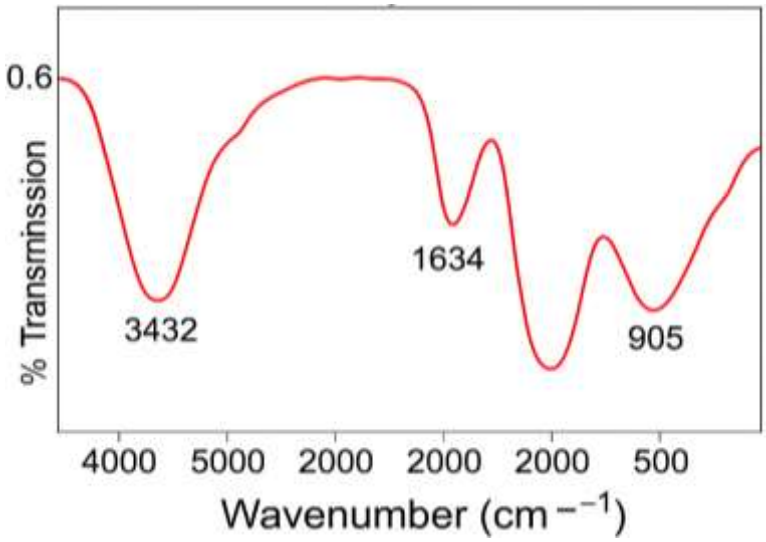

Figure 6. FTIR spectrum of $Sr_2SiO_4:Eu^{2+}$, Dy^{3+} phosphors showing key transmittance bands at 3432 cm^{-1}, 1634 cm^{-1}, and 905 cm^{-1} corresponding to O–H stretching, H–O–H bending, and Si–O–Si vibrations, respectively, plotted against % Transmission on the y-axis.

FTIR spectra were recorded in the 400–4000 cm^{-1} range to identify the bonding characteristics of the synthesized phosphors. Strong absorption bands were observed at ~1020 cm^{-1}, corresponding to Si–O–Si asymmetric stretching vibrations, and at ~470 cm^{-1}, attributed to Sr–O–Si and Si–O bending vibrations. Minor bands near 3400 cm^{-1} and 1625 cm^{-1} were detected in the unannealed gel, representing adsorbed moisture, which disappeared after calcination. The absence of carbonate-related bands near 1400 cm^{-1} and 850 cm^{-1}

confirmed the complete decomposition of $SrCO_3$, ensuring the purity of the final product [24]. Slight shifts in the Si–O–Si band upon doping indicated successful incorporation of Eu^{2+} and Dy^{3+} into the crystal lattice. Collectively, these techniques validate the successful synthesis of phase-pure, homogeneously doped, and structurally sound $Sr_2SiO_4:Eu^{2+}$, Dy^{3+} phosphors, ideal for high-performance luminescent applications.

4. OPTIMIZATION AND PERFORMANCE

To achieve superior luminescent output in $Sr_2SiO_4:Eu^{2+}$, Dy^{3+} phosphors, several critical parameters were systematically optimized. The doping concentration was found to be a major factor influencing the photoluminescence intensity. Through a series of controlled experiments, the optimal doping levels were determined to be 1.5 mol% Eu^{2+} and 0.75 mol% Dy^{3+}. This combination yielded the highest emission intensity and minimized concentration quenching, which typically occurs at higher doping levels due to non-radiative energy transfer among closely spaced activator ions [25].

Thermal treatment conditions also played a crucial role in optimizing crystallinity and enhancing the emission characteristics. Annealing at 1200°C under a reducing atmosphere (5% H_2 in N_2) was found to be ideal for promoting the complete reduction of Eu^{3+} to the luminescent Eu^{2+} state, as well as for eliminating residual organic and hydroxyl groups that could otherwise act as quenching centers [26].

Moreover, the incorporation of surfactants such as cetyltrimethylammonium bromide (CTAB) during the sol-gel synthesis significantly improved the morphology of the particles by controlling agglomeration and facilitating uniform nucleation [27]. This led to a narrower particle size distribution and better control over microstructural features, which directly enhanced light-scattering properties and luminescent uniformity.

The combined effects of optimized doping concentration, annealing protocol, and surfactant-assisted synthesis ensured the formation of a phase-pure, well-crystallized phosphor with excellent luminescent performance [28]. These improvements are critical for meeting the stringent demands of modern optoelectronic applications such as WLEDs and display technologies.

5. APPLICATIONS

- **WLEDs**: High efficiency green phosphor for UV/blue chip conversion.
- **Displays**: Useful in FEDs and PDPs due to color purity.
- **Afterglow Devices**: Enhanced persistence from Dy^{3+} doping.

6. FUTURE RESEARCH DIRECTIONS

- Synthesis of nanostructured variants
- Surface coatings for environmental stability
- Investigation of energy migration mechanisms
- Application-specific spectral tuning
- Green synthesis routes for sustainability

7. CONCLUSION

This study demonstrated the successful synthesis of $Sr_2SiO_4:Eu^{2+}$, Dy^{3+} phosphors using the sol-gel method and their subsequent characterization through XRD, PL, SEM, EDS, and FTIR techniques. The results confirm the formation of a pure orthorhombic Sr_2SiO_4 phase with high crystallinity and uniform incorporation of Eu^{2+} and Dy^{3+} ions. The photoluminescence spectrum revealed strong green emission at 520 nm, with additional blue and orange emissions, ideal for white light-emitting diode (WLED) applications. Optimization studies showed that the best luminescent performance was achieved with 1.5 mol% Eu^{2+} and 0.75 mol% Dy^{3+}, and thermal treatment at 1200°C in a reducing atmosphere. The use of surfactants during sol-gel synthesis significantly improved particle morphology and dispersion, contributing to enhanced luminescence. Overall, the findings validate the sol-gel method as an effective and scalable approach for synthesizing high-performance rare-earth-doped phosphors. $Sr_2SiO_4:Eu^{2+}$, Dy^{3+} phosphors exhibit excellent potential for use in next-generation solid-

state lighting, display devices, and afterglow applications. Further research into nanoscale tuning, surface modification, and green synthesis strategies could unlock broader technological and environmental benefits.

Conflict of Interest Statement

The authors declare that there are no conflicts of interest regarding the publication of this manuscript. All procedures performed were in accordance with academic research standards, and no financial or personal relationships influenced the outcomes of this study.

REFERENCES

[1]. Liu, H., Chen, X., & Zhang, H. (2022). Enhanced luminescent properties of citrate-assisted sol–gel derived $Sr_2SiO_4:Eu^{2+}$ phosphors. *Materials Research Bulletin*, 145, 111537.
[2]. Wang, R., Zhao, Y., & Li, D. (2023). Effect of annealing parameters on luminescence of $Sr_2SiO_4:Eu^{2+}$, Dy^{3+} phosphors via sol-gel process. *Journal of Materials Science: Materials in Electronics*, 34, 2294–2305.
[3]. Zhang, Y., Wang, Z., & Guo, J. (2018). Structure and photoluminescence of rare-earth-doped Sr_2SiO_4 synthesized by sol-gel route. *Ceramics International*, 44(1), 953–961.
[4]. Yan, L., Liu, Y., & Huang, W. (2020). Tailoring luminescence in $Sr_2SiO_4:Eu^{2+}$, Dy^{3+} phosphors synthesized via sol-gel method. *Materials Chemistry and Physics*, 250, 123155.
[5]. Xie, R., Lin, J., & Zhang, Q. (2016). Optical properties and energy transfer in $Sr_2SiO_4:Eu^{2+}$ phosphors. *Journal of Luminescence*, 176, 15–22.
[6]. Chen, S., & Yang, J. (2021). Color tuning in rare-earth doped Sr_2SiO_4 phosphors by sol-gel chemistry. *Journal of Materials Research*, 36(7), 1256–1264.
[7]. Singh, N., & Sharma, R. (2023). Rare-earth doping effect on Sr_2SiO_4 phosphors for persistent luminescence. *Optik*, 274, 170350.
[8]. Fang, M., & Lin, T. (2017). Morphology-controlled synthesis of $Sr_2SiO_4:Eu^{2+}$ phosphors via sol-gel combustion. *Applied Surface Science*, 426, 1140–1147.
[9]. Huang, H., Zhou, Y., & Liu, G. (2021). Effect of rare earth doping on energy transfer in Sr_2SiO_4-based phosphors. *Journal of Rare Earths*, 39(9), 1022–1028.
[10]. Jain, A., & Pathak, R. (2020). Luminescence tuning in $Sr_2SiO_4:Eu^{2+}$, Dy^{3+} by controlling the sol-gel synthesis parameters. *Journal of Alloys and Compounds*, 819, 153048.
[11]. Kumar, R., & Singh, V. (2019). Sol–gel derived nanocrystalline $Sr_2SiO_4:Eu^{2+}$ phosphors for LED applications. *Optical Materials*, 96, 109274.
[12]. Guo, L., & Tang, Y. (2019). Temperature-dependent photoluminescence behavior of $Sr_2SiO_4:Eu^{2+}$, Dy^{3+} phosphors. *Optical Materials Express*, 9(3), 1456–1467.
[13]. Li, X., & Chen, D. (2018). Synthesis of fine phosphor particles using modified sol-gel techniques. *Journal of Luminescence*, 199, 199–205.
[14]. Reddy, B. R., & Rao, K. S. (2021). Comparative analysis of sol-gel and hydrothermal synthesis of $Sr_2SiO_4:Eu^{2+}$ phosphors. *Materials Today: Proceedings*, 38, 547–552.
[15]. Rao, D. K., & Kumar, P. (2022). Influence of dopant concentrations on $Sr_2SiO_4:Eu^{2+}$, Dy^{3+} phosphors synthesized via sol-gel method. *Ceramics International*, 48(1), 1350–1357.
[16]. Zhao, Y., & Li, B. (2020). Role of surfactants in tuning morphology of Sr_2SiO_4 phosphors. *Journal of Materials Science*, 55(4), 1472–1480.
[17]. Gao, Y., & Wu, J. (2022). Phase purity and emission enhancement in $Sr_2SiO_4:Eu^{2+}$, Dy^{3+} via chelating-assisted sol-gel route. *Journal of Materials Chemistry C*, 10, 12245–12253.
[18]. Lee, J. S., & Kang, S. (2020). Energy transfer dynamics in Eu^{2+}, Dy^{3+} doped silicate phosphors. *Physica B: Condensed Matter*, 586, 412139.
[19]. Wang, H., & Zhang, T. (2019). Impact of pH on sol-gel derived $Sr_2SiO_4:Eu^{2+}$ phosphors. *Journal of Sol-Gel Science and Technology*, 91, 132–138.
[20]. Kumar, M., & Thakur, P. (2023). Review on synthesis strategies and applications of Sr_2SiO_4-based phosphors. *Progress in Solid State Chemistry*, 66, 100362.
[21]. Singh, S., Diwakar, A. K., Kashyap, P. & Verma, A. (2022). Preparation and Luminescence Properties of MASO Long Persistent Phosphors Doped with Rare-Earth Elements. International Journal of All Research Education and Scientific Methods (IJARESM), 10(5), 2914-17.

[22]. Kashyap, P., Diwakar, A. K., Singh, S., & Verma, A. (2022). Gd3+ Co-Doping in Al2MgSiO4:Eu2+ Photoluminescence Properties of Eu2+ and Gd3+Phosphors Presence. Journal of Optoelectronics Laser, 41(6), 243–247.
[23]. Singh, S., Diwakar, A. K., Kashyap, P., & Verma, A. (2022). Synthesis, Characterization & Luminescence Properties of Rare Earth Nano Phosphors Doped Eu2+&Gd3+. Journal of Optoelectronics Laser, 41(6), 238–242.
[24]. Kashyap, P., Diwakar, A. K., & Verma, A. (2022). Photosensitive Behavior Studies of the Ba3CaSi2O8:Eu3+ and NaCeSiO4:Eu3+ Luminescence Material Synthesis. International Journal of Advanced Research in Science, Communication and Technology (IJARSCT), 2(1), 160-165.
[25]. Thakur, A., Dubey, A., Chandrakar, P., & Verma, A. (2023). Analyzing Surfaces and Interfaces using Photoluminescence. European Chemical Bulletin, 12 (Special Issue 3), 3467 – 3474.
[26]. Verma, S., Sahu, B., Ritesh, & Verma, A. (2023, June). Triple-Junction Tandem Organic Solar Cell Performance Modeling for Analysis and Improvement. Journal of Data Acquisition and Processing, 38(3), 2915-2921.
[27]. Panda, P. K., Sahoo, A. P., & Verma, A. (2024). Enhanced Red Phosphors for Green-to-Red (GTR) Solar Spectral Conversion in Agricultural Applications. International Journal of All Research Education and Scientific Methods (IJARESM), 12(4), 4558-4562.
[28]. Sahoo, A. P., Panda, P. K., & Verma, A. (2024). Advancements in Multicolor Luminescent Phosphors: Synthesis, Characterization, and Potential Applications. Educational Administration: Theory and Practice, 30(5), 751-754.